

The Local Group: The Ultimate Deep Field

Michael Boylan-Kolchin^{1*}, Daniel R. Weisz^{2†}, James S. Bullock³,
Michael C. Cooper³

¹Department of Astronomy, The University of Texas at Austin, 2515 Speedway, Stop C1400, Austin, TX 78712-1205, USA

²Astronomy Department, Box 351580, University of Washington, Seattle, WA 98195, USA

³Department of Physics and Astronomy, University of California at Irvine, Irvine, CA 92697, USA

13 February 2022

ABSTRACT

Near-field cosmology – using detailed observations of the Local Group and its environs to study wide-ranging questions in galaxy formation and dark matter physics – has become a mature and rich field over the past decade. There are lingering concerns, however, that the relatively small size of the present-day Local Group (~ 2 Mpc diameter) imposes insurmountable sample-variance uncertainties, limiting its broader utility. We consider the evolution of the Local Group with time and show that it reaches $3' \approx 7$ co-moving Mpc in linear size (a volume of ≈ 350 Mpc³) at $z = 7$. The Local Group is a representative portion of the Universe at early cosmic epochs according to multiple metrics. In a sense, the Local Group is therefore the ultimate deep field: its stellar fossil record traces the cosmic evolution for galaxies with $10^3 \lesssim M_*(z=0)/M_\odot \lesssim 10^9$ (reaching $m_{1500} > 38$ at $z \sim 7$) over a region that, in terms of size, is comparable to or larger than the *Hubble* Ultra-Deep Field (HUDF) for the entire history of the Universe. It is highly complementary to the HUDF, as it probes *much* fainter galaxies but does not contain the intrinsically rarer, brighter sources that are detectable in the HUDF. Archaeological studies in the Local Group also provide the ability to trace the evolution of individual galaxies across time as opposed to evaluating statistical connections between temporally distinct populations. In the *JWST* era, resolved stellar populations will probe regions larger than the HUDF and any deep *JWST* fields, further enhancing the value of near-field cosmology.

Key words: cosmology: theory, observations – galaxies: evolution – Local Group

1 INTRODUCTION

The standard introduction of a paper on near-field cosmology extols the virtues of the Local Group as a cosmic Rosetta Stone that provides archaeological clues left behind by untold generations of stars, clues that may unlock unsolved mysteries in galaxy formation. A frequent concern is that resolved-star studies are inherently limited to a region that is relatively small and likely biased, however, setting fundamental limits on the broader applicability of results based on near-field studies. In this *Letter*, we show that the volume spanned by the high-redshift progenitors of the Local Group was large enough to have been typical in many respects. The archaeological record imprinted on Local Group galaxies is therefore likely to provide an unbiased view of faint galaxy populations at early times, making near-field observations a powerful complement to direct deep-field studies.

2 METHODS

At present, the Local Group consists of two dark matter halos, each with virial mass of $\sim 10^{12} M_\odot$ (e.g., Klypin et al. 2002), approaching each other for presumably the first time (Kahn & Woltjer 1959). The co-moving Lagrangian volume of the matter contained within the Local Group – i.e., the co-moving volume spanned at earlier epochs by the particles in the current-day Local Group – was therefore larger in the past; the same is true for all dark matter halos. Thus, while the Local Group is a very specific (and non-typical) volume of the Universe today, its properties at earlier times should be closer to an average portion of the Universe. Precisely how much closer is the topic of this paper.

A starting point for understanding the evolution of the Local Group with time is the spherical collapse model (Gunn & Gott 1972), in which the radius of the Local Group at maximum expansion was approximately twice as large as it is at the present day. However, this underestimates the size of the Local Group’s Lagrangian volume at earlier times, predominantly because of the non-spherical nature of grav-

* mbk@astro.as.utexas.edu

† Hubble Fellow

itational collapse in an expanding Universe. Cosmological zoom-in simulations, by design, supply a way of following the evolution of Lagrangian regions surrounding specific halos from linear fluctuations to the highly non-linear regime (see Oñorbe et al. 2014 for a discussion of this technique, which was originally described in Katz & White 1993, and for examples of the evolution of Lagrangian volumes with redshift). The ELVIS suite of N -body zoom-in simulations (Garrison-Kimmel et al. 2014) provides 12 Local Group analogs simulated from $z = 125$ to $z = 0$, each of which is uncontaminated by lower resolution particles over a spherical region having a radius of at least 1.2 Mpc centered on the $z = 0$ barycenter of the Local Group. In what follows, we use this suite to study the co-moving volume probed by the Local Group at higher redshifts.

In our analysis, we first eliminate three ELVIS pairs that contain a third large, nearby halo, as these would bias any results. For the remaining 9 pairs, we identify all subhalos within 1.2 Mpc of the Local Group’s $z = 0$ barycenter and track *all* of their progenitors back through time. There are occasionally individual subhalos that come from regions that are distant from the vast majority of the matter that forms the Local Group; such subhalos can artificially increase the inferred volume of the Local Group at earlier times. To eliminate these objects, we run a friends-of-friends (Davis et al. 1985) group finder with a large linking length of 400 kpc and retain only the main grouping. In practice, this removes $\ll 1\%$ of subhalos at $z = 0$. We then identify the positions spanned by the progenitors of the remaining Local Group subhalos above the ELVIS completeness limit of $M_{\text{peak}} = 6 \times 10^7 M_{\odot}$ at each earlier snapshot; this constitutes the “proto-Local-Group” at each epoch. It is important to note that the number of galaxies or halos in the proto-Local-Group is much larger than the number in the Local Group at $z = 0$ owing to mergers and disruption over time.

If we are only interested in understanding the Local Group itself, this would be sufficient. To place the Local Group in context at higher redshifts, however, we must understand the full environment that the proto-Local-Group occupies. We therefore compute, at each snapshot, the minimum cuboid volume defined by the proto-Local-Group – i.e., the rectangular cuboid defined by the minimum and maximum co-moving coordinate locations of all proto-Local-Group progenitors at that time, \mathcal{V}_{RC} – and identify all additional halos in this region (i.e., halos that appear to be part of the proto-Local-Group but that do not end up in the Local Group at $z = 0$). The inclusion of these objects roughly doubles the counts at $z \sim 7$ within \mathcal{V}_{RC} , with proto-Local-Group halos dominating the central portion of \mathcal{V}_{RC} and the additional halos populating the outskirts of the volume.

We define the linear size of the proto-Local-Group $l_{\text{LG}}(z)$ as the geometric mean of the three axes defining $\mathcal{V}_{\text{RC}}(z)$; in other words, $l_{\text{LG}}(z) = \mathcal{V}_{\text{RC}}(z)^{1/3}$. At $z = 0$, the Local Group volume is defined by a sphere of radius 1.2 Mpc, so $l_{\text{LG}}(z = 0) \approx 2.4$ Mpc (the actual number depends on the distribution of halos at $z = 0$ but can never exceed 2.4 Mpc). At higher redshifts, \mathcal{V}_{RC} can, in principle, become highly elongated in one or two dimensions. In practice, however, we find that this is not the case: at $z = 7$, the median minor-to-major axis ratio is 0.76 and the median intermediate-to-major axis ratio is 0.81, and in only one case is the minor axis smaller than half of the major

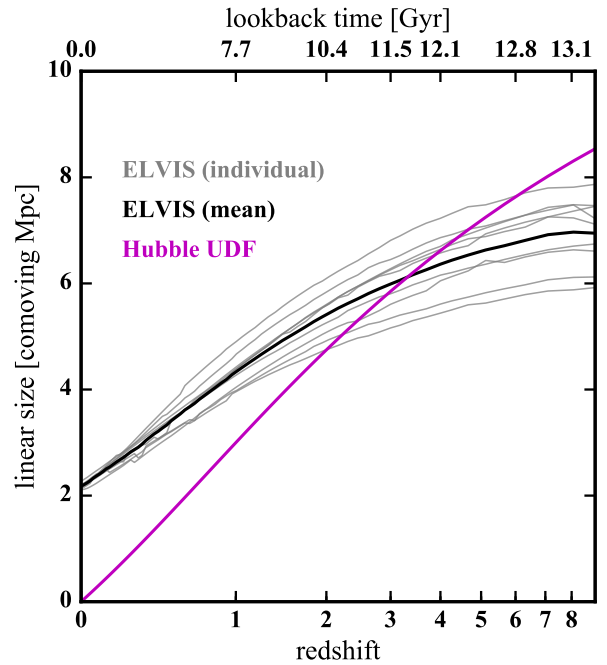


Figure 1. The co-moving linear extent of the proto-Local-Group (black, gray curves) and HUDF (magenta curve) as a function of redshift. For $z \lesssim 3$, the proto-Local-Group covers an area on the sky that is larger than the HUDF. At earlier times, the HUDF is marginally larger. The typical proto-Local-Group reaches a co-moving size of 7 Mpc at $z \sim 7$, meaning it probes an effective volume of ~ 350 co-moving Mpc^3 in the reionization era.

axis size. The typical $\mathcal{V}_{\text{RC}}(z = 7)$ is moderately prolate: 6 of 9 simulated proto-Local-Groups have a triaxiality parameter T (see Franx et al. 1991) larger than 0.5.

3 THE LOCAL GROUP THROUGH TIME

Figure 1 shows the co-moving linear size, $l_{\text{LG}}(z)$, of the proto-Local-Group going back in time to $z = 9$. Thin gray lines show the size of individual LG pairs from the ELVIS simulation suite, while the thick black line shows the median value across the ELVIS pairs at each redshift. The linear size of the proto-Local-Group increases with increasing redshift, reaching ≈ 7 Mpc (co-moving) at $z \sim 7$. Going back in time, therefore, the Local Group probes a significantly larger (co-moving) volume than it does today. To give context to the Local Group’s size at earlier epochs, Fig. 1 also shows the co-moving linear size of the HUDF (Beckwith et al. 2006, assuming an angular size of $3.1' \times 3.1'$) as a function of redshift (magenta curve). *At all epochs later than $z \approx 3$ (the last 85% of cosmic time), the proto-Local-Group covers a larger area on the sky than the HUDF.*

It is important to understand how representative such portions of the Universe are at each cosmological epoch. One way to do this is to compute the rms amplitude of density fluctuations σ in regions having volumes equal to $\mathcal{V}_{\text{RC}}(z)$. In classical Press-Schechter (1974) theory and its extensions, the typical scale M^* that is collapsing at a given epoch has $\sigma_{\text{lin}}(M^*, z) = \delta_c \approx 1.686$ (where subscript “lin” indicates that the relevant rms amplitude comes from linear theory,

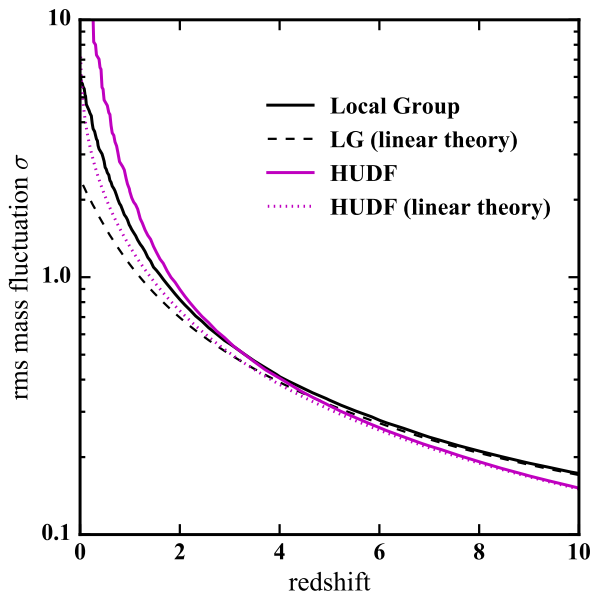


Figure 2. The rms mass fluctuation, σ , computed over volumes equal to that covered by the proto-Local-Group (black) and HUDF (magenta) as a function of redshift. Also shown are linear theory values for σ over those same volumes. At early times, both regions have $\sigma \sim 0.2$ and the redshift evolution is well-described by linear theory. The regions become non-linear ($\sigma \gtrsim 1$) at $z \sim 2$, by which point linear theory underestimates the true rms amplitude of fluctuations.

extrapolated to the redshift in question). Roughly speaking, scales with $\sigma(M, z) \gg 1$ have collapsed while those with $\sigma(M, z) \ll 1$ are firmly in the linear regime.

In reality, linear theory underestimates $\sigma(M, z)$. Cosmological simulations account for effects of non-linear growth; accordingly, we use the *Illustris* suite (Vogelsberger et al. 2014b,a; Nelson et al. 2015) to compute $\sigma(M, z)$. At each snapshot, we evaluate the density field for *Illustris*-Dark-1 on a 256^3 grid, compute the overdensity $\delta_i = \rho_i / \langle \rho \rangle - 1$ for each cell i , then calculate $\delta(M, z)$ by smoothing the gridded overdensity field with a real-space top-hat filter having a volume equal to $\mathcal{V}_{\text{RC}}(z)$ (so the mass contained in the volume is $M_{\text{LG}} = \rho_m(z) \mathcal{V}_{\text{RC}}(z)$). The rms amplitude of fluctuations is therefore equivalently characterized by $\sigma(M_{\text{LG}}, z)$ or $\sigma(l_{\text{LG}}, z)$.

The resulting values for $\sigma(l_{\text{LG}}, z)$ are plotted as a solid black curve in Figure 2; the linear theory value of $\sigma(l_{\text{LG}}, z)$ is shown as a dashed black curve. We also compute the same quantities for the HUDF, $\sigma(l_{\text{HUDF}}, z)$, and plot these with magenta curves. Both the Local Group and the HUDF have $\sigma < 1$ for $z \gtrsim 2$. At high redshift, both probe volumes that are well-described by linear theory. In particular, the volumes probed by the proto-Local-Group and by cubic slices of the HUDF ($\Delta z \approx 0.02$) in the reionization era ($6 \lesssim z \lesssim 10$) have $\sigma(M_{\text{LG}}) \lesssim 0.25$. For a broad discussion of variance in deep-field galaxy counts, see Robertson (2010).

The results above have established that the proto-Local-Group was substantially larger at earlier epochs, large enough to cover a volume that becomes non-linear only after $z \sim 2$. A further, and more stringent, test is to compare the mass function in the region defined by the proto-

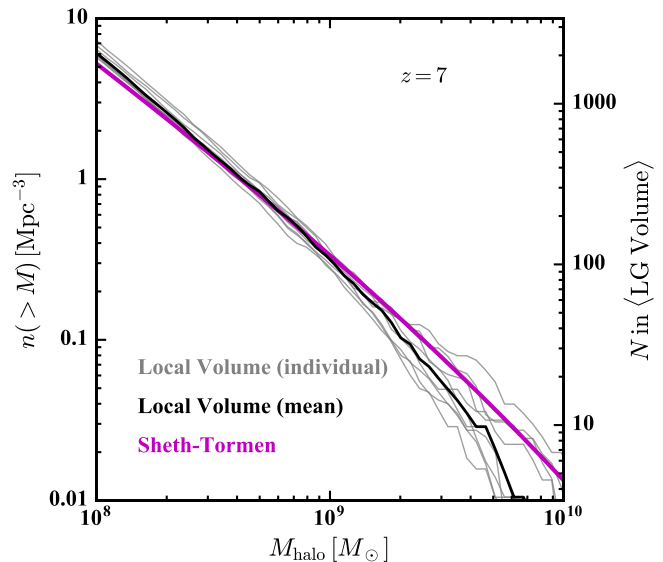


Figure 3. Cumulative dark matter halo mass functions for the volume spanned by the proto-Local-Group at $z = 7$ (gray curves: individual ELVIS simulations; black curve: ensemble average). The right y-axis gives the cumulative counts for the average proto-Local-Group region in ELVIS. The magenta curve shows the global Sheth-Tormen mass function. At $z = 7$, the normalization of the ELVIS proto-Local-Group mass function agrees very well with the Sheth-Tormen mass function, indicating the proto-Local-Group covers a representative portion of the Universe.

Local-Group to the cosmological mass function at earlier times. In Figure 3, we plot the cumulative co-moving number density $n(> M)$ of halos within \mathcal{V}_{RC} for each ELVIS pair (thin gray lines), as well as the median across the simulation suite (thick black line), at $z = 7$. The cosmological expectation, as encapsulated by the Sheth-Tormen (2001) mass function, is plotted as a magenta line. The mass function in $\mathcal{V}_{\text{RC}}(z = 7)$ matches the cosmological mass function for $M_{\text{vir}} \lesssim 2 \times 10^9 M_{\odot}$, with counts in the proto-Local-Group region falling below Sheth-Tormen at higher masses (smaller number densities) owing to the size of this region. *The volume covered by the proto-Local-Group at $z = 7$ is therefore a cosmologically representative region for the mass function of halos with $M_{\text{vir}}(z = 7) \lesssim 2 \times 10^9 M_{\odot}$, a remarkable result.*

As indicated by the scale on the right side of the figure, there should be ~ 2000 halos with $M_{\text{vir}} > 10^8 M_{\odot}$ (this approximately corresponds to halos above the atomic cooling threshold) and ~ 100 halos with $M_{\text{vir}} > 10^9 M_{\odot}$ in the $z = 7$ proto-Local-Group region. It is this large number of low-mass systems, coupled with the small value of $\sigma(l_{\text{LG}}, z = 7)$, that makes mass functions in the proto-Local-Group cosmologically representative even in the 350 Mpc^3 co-moving volume at early times (note the small variance in normalizations of the mass functions in Fig. 3).

By $z = 4$, the proto-Local-Group has become somewhat more dense, and the equivalent plot of mass functions shows that counts in the proto-Local-Group volume exceed Sheth-Tormen expectations by $\approx 50\%$ at this epoch. However, the shape of the mass functions still matches that of Sheth-Tormen for cumulative number densities larger than 10^{-2} Mpc^{-3} (equivalently, $M_{\text{vir}} < 5 \times 10^{10} M_{\odot}$).

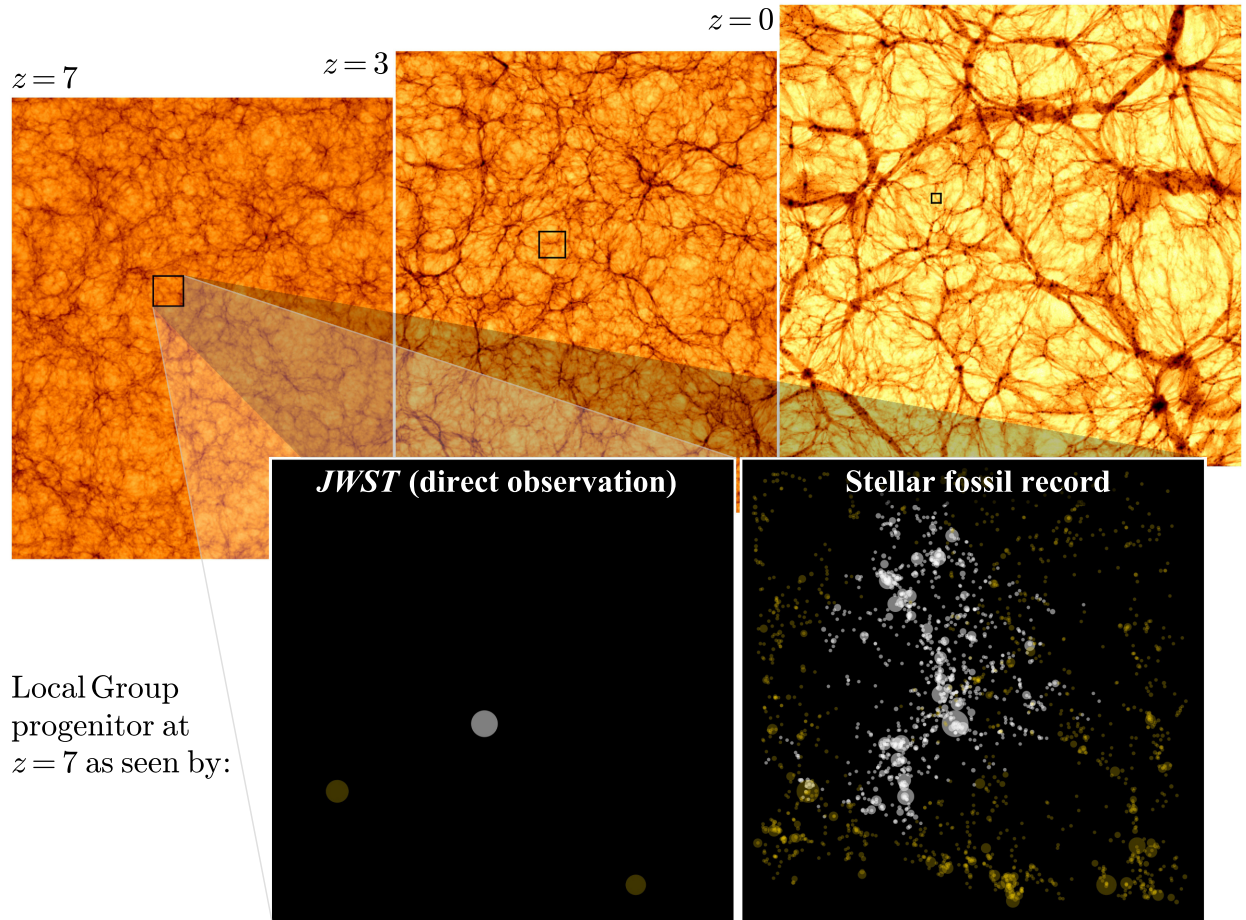


Figure 4. Density slices of the *Illustris* simulation at $z = 0, 3,$ and 7 (upper panels; side length of 106.5 co-moving Mpc), along with the co-moving size of the average proto-Local-Group at each redshift (top panels). The bottom panels show the galaxies in such a region (which is comparable in linear extent to the HUDF) that are accessible at $z = 7$ through direct observation with *JWST* in a narrow redshift slice of width $\Delta z \approx 0.02$ (corresponding to the ~ 7 Mpc co-moving size of the proto-Local-Group at $z = 7$) and through the stellar fossil record in the Local Group. White symbols indicate objects that end up in the Local Group at $z = 0$, while gold symbols represent objects in the proto-Local-Group volume at $z = 7$ but not within 1.2 Mpc of the Local Group barycenter at $z = 0$.

4 DISCUSSION

The similarity between the (1D) size of the proto-Local-Group and the HUDF suggests an interpretation of the Local Group at earlier epochs: *observations of the Local Group can be thought of as providing a (very) narrow slice in time of the HUDF*. Given our ability to measure resolved star formation histories of Local Group galaxies, we can look at the Local Group at a variety of “snapshots” in time. This is therefore the same as looking at a series of thin transverse slices through the HUDF. A complete census of galaxies within 1–2 Mpc of the Local Group with depth to reach the oldest main sequence turn-off would therefore allow a *continuous* look at galaxy formation and evolution – i.e., tracking individual galaxies across cosmic time – in a size equivalent to the HUDF to depths of $m \sim 38$ ($M_{UV} \approx -9$) at $z = 7$.

We emphasize that resolved-star studies of the Local Group provide an almost perfectly complementary view of galaxy formation to deep blank-field (and lensing) observations of the high-redshift Universe with *Hubble*. At $z \sim 7$, the faintest galaxies in blank-field *HST* observations are likely

to be more massive than the progenitor of the Milky Way at that time (Boylan-Kolchin et al. 2014). Archaeological studies of Local Group galaxies extend the range of galaxies to at least 8 magnitudes fainter (Weisz et al. 2014; Boylan-Kolchin et al. 2015; Graus et al. 2016). *HST* is therefore capable of probing galaxy formation over six decades in mass ($10^3 < M_*/M_\odot < 10^9$) and 12–13 Gyr in time over an area comparable to the HUDF via the stellar fossil record.

The power of near-field studies, and their complementarity to direct high- z observations, is emphasized in Figures 4 and 5. For both figures, we assign UV luminosities at $z = 7$ to ELVIS dark matter halos via abundance matching based on the global UV luminosity function from Finkelstein et al. (2015) and the Sheth-Tormen mass function. Figure 4 shows slices through the density distribution of the *Illustris* simulation at $z = 0, 3,$ and 7 , along with boxes indicating the approximate size of the proto-Local-Group at each of those redshifts. The insets at $z = 7$ show galaxies that can be observed either directly in the proto-Local-Group with the *James Webb Space Telescope* (*JWST*; left) or through archaeological studies in the Local Group with *HST* (right).

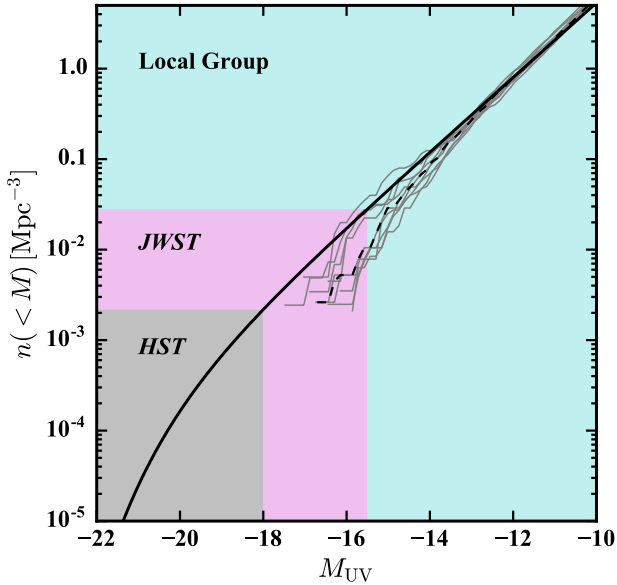


Figure 5. Complementarity of direct observation and stellar fossil record studies of galaxies at high- z . *Solid line*: cumulative luminosity function at $z \sim 7$ from deep-field observations using *HST* (from Finkelstein et al. 2015). The best-fitting cumulative luminosity function is extrapolated beyond the HUDF magnitude limit of $M_{UV} = -18$. *Solid gray curves* show the cumulative luminosity functions found in each ELVIS pair based on abundance matching. The agreement in normalization between the luminosity function globally and in the proto-Local-Group region is a direct result of the unbiased nature of counts in the proto-Local-Group volume at $z = 7$ (Fig. 3). The approximate blank field limiting magnitude for *JWST* is also shown, along with the corresponding number density. The Local Group probes galaxies that, for the most part, will remain undetected through direct observations in the high- z Universe because of their intrinsic faintness.

JWST deep fields will have many more galaxies at a range of redshifts, while the stellar fossil record in the Local Group probes a huge number of galaxies that will be unobservably faint at cosmic dawn.

Fig. 5 shows the cumulative galaxy luminosity function from Finkelstein et al. (2015) at $z = 7$ (thick black curve), extrapolated from the *HST* observational limit of $M_{UV} \sim -18$ all the way to $M_{UV} = -10$. Each gray line shows the luminosity function in the proto-Local-Group volume from an individual ELVIS simulation, while the dashed black line shows the mean among all ELVIS pairs. *Note that the agreement in normalization between the global luminosity function and the proto-Local-Group regions from ELVIS was not pre-determined but rather is a result of the agreement between the global halo mass function and the halo mass function within the proto-Local-Group at $z = 7$.* The approximate reach of *HST* and *JWST* is shown in the figure, while the proto-LG covers the entire region of the figure in which the halo mass functions are non-zero.

The high angular resolution of *JWST* and its exquisite sensitivity to (red) ancient main sequence turn-off stars make it ideally suited to extend the same census to 3–5 Mpc, meaning it is capable of surveying a region within the Local Volume that is markedly larger than the HUDF (and any *JWST* deep field) at all redshifts. The complementarity

with direct observations of galaxies at early cosmic epochs will also be enhanced, as *JWST* will likely detect galaxies as faint as $M_{UV} \sim -15.5$ in blank fields at $z \sim 7$ (Windhorst et al. 2006), comparable to progenitors of the Large Magellanic Cloud (Boylan-Kolchin et al. 2015). The *Wide-Field Infrared Survey Telescope* (*WFIRST*) has potential to be similarly transformative for near-field cosmology. The addition of an optical filter (e.g., *R*-band) would improve its angular resolution (and temperature sensitivity), allowing it to reach the ancient main sequence turn-offs of galaxies out to ~ 5 Mpc. This modification, combined with *WFIRST*’s extremely wide field of view, would capture full star formation histories over the entire spatial extent of virtually any nearby galaxy in a single pointing, revolutionizing how we study and understand the evolution of low-mass galaxies.

ACKNOWLEDGMENTS

We thank Mark Vogelsberger and Lars Hernquist for assistance with accessing and analyzing *Illustris* data via the Odyssey cluster, which is supported by the FAS Division of Science Research Computing Group at Harvard University. MBK acknowledges support from NSF grant AST-1517226 and from NASA grants HST-AR-12836 and HST-AR-13888 awarded by STScI. D.R.W. is supported by NASA through Hubble Fellowship grant HST-HF-51331.01 awarded by STScI. JSB was supported by NSF-AST-1518291, HST-AR-14282, and HST-AR-13888. Much of the analysis in this paper relied on the python packages NumPy (Van Der Walt et al. 2011), SciPy (Jones et al. 2001), Matplotlib (Hunter 2007), and iPython (Pérez & Granger 2007), as well as pyfof (<https://pypi.python.org/pypi/pyfof/>); we are very grateful to the developers of these tools. This research has made extensive use of NASA’s Astrophysics Data System and the arXiv eprint service at arxiv.org.

REFERENCES

- Beckwith S. V. W., et al., 2006, *AJ*, **132**, 1729
 Boylan-Kolchin M., Bullock J. S., Garrison-Kimmel S., 2014, *MNRAS*, **443**, L44
 Boylan-Kolchin M., Weisz D. R., Johnson B. D., Bullock J. S., Conroy C., Fitts A., 2015, *MNRAS*, **453**, 1503
 Davis M., Efstathiou G., Frenk C. S., White S. D. M., 1985, *ApJ*, **292**, 371
 Finkelstein S. L., et al., 2015, *ApJ*, **810**, 71
 Franx M., Illingworth G., de Zeeuw T., 1991, *ApJ*, **383**, 112
 Garrison-Kimmel S., Boylan-Kolchin M., Bullock J. S., Lee K., 2014, *MNRAS*, **438**, 2578
 Graus A. S., Bullock J. S., Boylan-Kolchin M., Weisz D. R., 2016, *MNRAS*, **456**, 477
 Gunn J. E., Gott J. R. I., 1972, *ApJ*, **176**, 1
 Hunter J. D., 2007, *Computing In Science & Engineering*, **9**, 90
 Jones E., Oliphant T., Peterson P., et al., 2001, *SciPy: Open source scientific tools for Python*, <http://www.scipy.org/>
 Kahn F. D., Woltjer L., 1959, *ApJ*, **130**, 705
 Katz N., White S. D. M., 1993, *ApJ*, **412**, 455
 Klypin A., Zhao H., Somerville R. S., 2002, *ApJ*, **573**, 597
 Nelson D., et al., 2015, *Astronomy and Computing*, **13**, 12
 Oñorbe J., Garrison-Kimmel S., Maller A. H., Bullock J. S., Rocha M., Hahn O., 2014, *MNRAS*, **437**, 1894
 Pérez F., Granger B. E., 2007, *Computing in Science and Engineering*, **9**, 21

- Press W. H., Schechter P., 1974, *ApJ*, **187**, 425
Robertson B. E., 2010, *ApJ*, **713**, 1266
Sheth R. K., Mo H. J., Tormen G., 2001, *MNRAS*, **323**, 1
Van Der Walt S., Colbert S. C., Varoquaux G., 2011,
arXiv:1102.1523 [astro-ph],
Vogelsberger M., et al., 2014a, *MNRAS*, **444**, 1518
Vogelsberger M., et al., 2014b, *Nature*, **509**, 177
Weisz D. R., Johnson B. D., Conroy C., 2014, *ApJ*, **794**, L3
Windhorst R. A., Cohen S. H., Jansen R. A., Conselice C., Yan
H., 2006, *New Astron. Rev.*, **50**, 113